



Blistering of the selected materials irradiated by intense 200 keV proton beam

V.T. Astrelin^{a,b}, A.V. Burdakov^{a,c}, P.V. Bykov^a, I.A. Ivanov^{a,b}, A.A. Ivanov^{a,b}, Y. Jongen^d, S.G. Konstantinov^a, A.M. Kudryavtsev¹, K.N. Kuklin^a, K.I. Mekler^a, S.V. Polosatkin^{a,b,*}, V.V. Postupaev^{a,b}, A.F. Rovenskikh^a, S.L. Sinitskiy^{a,b}, E.R. Zubairov^a

^a Budker Institute of Nuclear Physics, Lavrent'eva 11, Novosibirsk 630090, Russia

^b Novosibirsk State University, Novosibirsk, Russia

^c Novosibirsk State Technical University, Novosibirsk, Russia

^d Ion Beam Applications SA, Louvain-la-Neuve, Belgium

ARTICLE INFO

Article history:

Received 14 April 2009

Accepted 13 October 2009

ABSTRACT

Formation of blisters on the surfaces of metal targets made of the selected materials was studied. The targets were irradiated by 100–200 keV, 1–2 mA proton beam up to the doses above 10^{24} m^{-2} . Real-time monitoring of the target surface was performed with a set of in situ optical surface diagnostics that allows detection of the moment of blisters appearance.

The overview of experimental setup and the results of testing of different materials are presented. The number and the size of blisters gradually increase during the irradiation. Critical fluence of blistering strongly depends on the target temperature, proton energy and surface machining method. The features of blistering under the proton beam irradiation and the effects of hydrogen diffusion and interaction with the target lattice are discussed.

© 2009 Elsevier B.V. All rights reserved.

1. Introduction

One of the known effects of radiation damage of materials is blistering, which results in modification of physical properties of the irradiated surface and in the increased erosion rate. Extensive studies of blistering were carried out with helium beams (see, e.g. review [1,2] and the references therein), this is the simplest case for the discussed phenomenon due to a chemical inertness of helium. The model that quantitatively describes blistering and the related processes exists [3]. The comprehensive review of experiments and theoretical models of blistering on different targets for helium and hydrogen beams was presented in [2]. At the same time most of the data concern with irradiation of the targets by helium or low-energy (about 5 keV/amu) hydrogen beams. Experimental database on blistering phenomena for high-energy beams of hydrogen isotopes is scarcer. On the other hand, several important applications depend on the surface stability (i.e. absence of blistering) under high-fluence, high-power, high-energy beams, for which the existing knowledge base is not sufficient. Grids of ion optics and beam dumps of high-power neutral beam injectors for large fusion facilities are some of the examples. Another application, which is of interest for our group, is the long-lifetime neutron-generating target for boron-neutron cancer therapy (BNCT)

facility (see, e.g., [4,5]). Such target should be composed of $\sim 1 \mu\text{m}$ lithium layer on the metal substrate. The target is irradiated by an intense 2 MeV proton beam and should survive the fluence of up to 10^{24} m^{-2} . Radiation damage of the lithium-substrate boundary will degrade the heat removal from front lithium surface that will result in overheating of the lithium layer. Therefore special experiments were performed to select blistering-resistant materials for the target substrate and to estimate the target lifetime.

The threshold of blistering formation under proton beam irradiation is closely related to the ability of metals to dissolve hydrogen. Large fluence of hydrogen atoms can be absorbed by a few of the metals with negative energy of hydrogen dissolution. These are transition metals of III-B and V-B groups of the periodic table of the elements – La, V, Nb, Ta. Practically all other metals cannot accumulate more than a few percents of hydrogen and therefore other metals were not considered as candidate substrate material. The exceptions are palladium and pure iron, which possess a very high diffusivity of hydrogen that might lead to the drainage of hydrogen from the surface into the bulk of a target. Thus, the presented experiments were restricted only by irradiation of the targets made of Ta, V, Pd and Fe. Also the experiments with Cu and W were performed to study general properties of blistering effect and comparison of the received data with the results of other authors.

2. Stand for experimental study of blistering at $100 \div 200 \text{ keV}$

A special stand was developed and assembled to perform the investigation of the blistering effects caused by proton beam at

* Corresponding author. Address: Budker Institute of Nuclear Physics, Lavrent'eva 11, Novosibirsk 630090, Russia. Tel.: +7 3833294773; fax: +7 383307163.

E-mail address: s.v.polosatkin@inp.nsk.ru (S.V. Polosatkin).

¹ Deceased author.

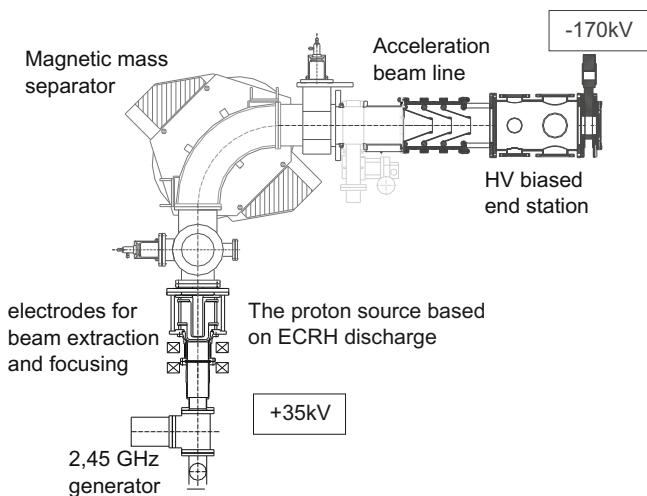


Fig. 1. Layout of the test stand.

the surfaces of metals. The layout of the stand is shown in Fig. 1. It comprises the primary ECR discharge ion source with a 35 keV primary beam energy, a mass separating magnet, a sectioned post-acceleration tube, and a high-voltage-biased end station with target arrangements and diagnostics.

The stand is supposed to provide generation of a proton beam with energy up to 200 keV and current up to 2 mA in the continuous mode. The current density at the target was up to 15 A/m². In the discussed experiments, the maximum fluence was 7×10^{24} protons/m².

The targets were cooled from the back side. In this paper, we will refer the temperature of the coolant as the target temperature. This means that the actual front surface temperature is higher. No recalculation for the temperature of the front surface has been performed because this quantity depends on the already accumulated radiation damage. As is known, caps of blisters and flakes lose thermal contact with the target body and, therefore, become overheated under intensive beams. An additional consequence of this overheating is the degradation of mechanical strength of non-heat-resistant materials that can lead to a lower threshold of blistering as compared with the irradiation by low-power beams. In the discussed experiments, the target temperature can be varied in the range from room temperature to 100 °C by control of the coolant temperature.

A set of real-time optical diagnostics was used to monitor the changes in optical properties of the front target surface during irradiation. The targets were generally prepared for the experiments with the optical-quality mirror surface processed by diamond cutting or fine polishing. Growth of blisters on a flat surface can be considered as the increase of surface roughness that causes the decrease of mirror reflectivity and increase of the scattered (diffusively reflected) light intensity.

During the experiments, the targets were illuminated at 30° glancing angle of incidence of a light beam. The appearance of blisters was monitored by intensities of the light reflected from the target surface and scattered at low (7°) and high (90°) angles. In practice, the intensities of mirror reflection and of diffusively reflected light gradually changed during the irradiation due to modification of optical properties of the target surface while the blistering caused fast changes in light intensities. Tungsten incandescent lamp and He-Ne laser were used as the sources of illumination.

3. Experimental study of blistering

Several candidate target materials were studied in the experiments. First targets were made from copper and tungsten – the

metals with the best known behavior under a high-fluence particle irradiation. These targets were used as a benchmark of our measurement techniques against the known reference data [6–8]. Other materials were candidates for a substrate of a long-lifetime target.

3.1. Copper targets

Several experiments with copper targets were carried out at temperatures of 296 and 370 K. The targets were made of the annealed oxygen-free copper of M0 grade (>99.97% Cu). The front target surface was processed by diamond cutting to a mirror quality. Scattered light intensity was used as a monitor of blister appearing. After irradiation the targets were studied by scanning electron microscopy (SEM) with a 100 nm spatial resolution.

The dynamics of the scattered light intensity for two experiments is shown in Fig. 2. Reproducibility of the experimental data with the targets of the same production batch was good. The diffusively reflected light starts changing gradually with some delay after the beginning of irradiation. There is a large fluence interval between the beginning of diffusively reflected light growth (which is associated with the appearance of the first blisters) and the maximum of scattered light (which corresponds to the developed blistering). Further increase of the irradiation fluence leads to some decrease of intensity of the diffusively reflected light that is caused by sluggish changes in the surface damage by blistering and/or by gradual changes of optical properties of the surface due to other processes.

A significant conclusion made from these experiments is the lack of sharp threshold for blistering. Rare small blisters were found on the surface of the target irradiated to 0.25×10^{22} m⁻² (label 1 in Figs. 2 and 3a). The surface irradiated to 2.6×10^{22} m⁻² becomes completely covered by blisters (label 2 in Figs. 2 and 3b). Between these two cases, gradual increase of the sizes and the surface density of blisters occur. Therefore, the term “threshold of blistering” for the discussed conditions is a matter of convention. From the practical point of view, the surface of Fig. 3a is almost undamaged and the surface of Fig. 3b is heavily modified. Therefore, practical threshold of blistering could be defined as the fluence, for which the blistering rate is maximal. This fluence practically coincides with that of the half-maximum increment of diffusive reflectance in respect to the reflection from a non-modified surface. Further in this paper, we will use the term “blistering threshold” as the fluence, which corresponds to the middle between the maximal and minimal intensities of the scattered light (this point is shown by the arrow in Fig. 2).

The experimental results for copper targets are shown in Fig. 4. Threshold fluence depends on the beam energy and the target

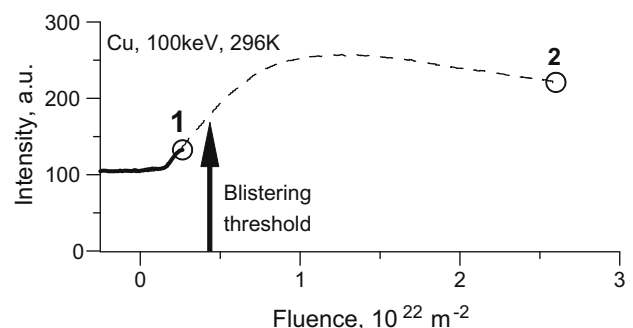


Fig. 2. Dynamics of scattered light intensity during the copper target irradiation in two similar experiments. Circles mark final fluence for each target. Parameters: beam energy 100 keV, temperature 296 K. Arrow indicates the fluence which was referred to as the threshold of blistering in this paper.

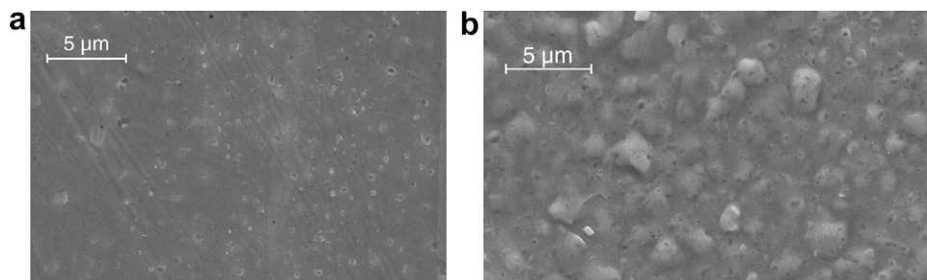


Fig. 3. SEM images of the irradiated copper targets; part (a) is for $E = 100$ keV, $T = 296$ K, fluence $0.25 \times 10^{22} \text{ m}^{-2}$ (label 1 in Fig. 2), start of blistering; part (b) is for $E = 100$ keV, $T = 296$ K, fluence $2.6 \times 10^{22} \text{ m}^{-2}$ (point 2 in Fig. 2), developed blistering.

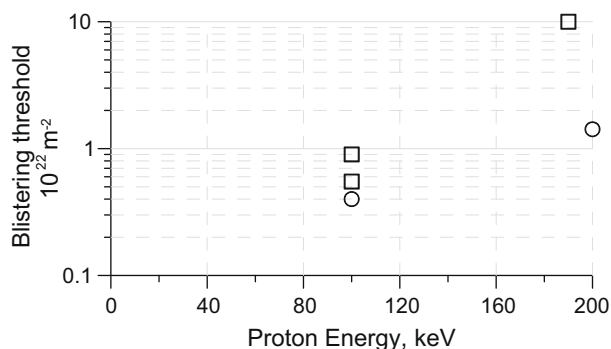


Fig. 4. Threshold of blistering on copper targets for different proton energies and target temperatures; circles are for $T = 296$ K, squares are for $T = 360$ K.

temperature. Almost all the data are for $10.5 \div 13 \text{ A/m}^2$ current density except for 200 keV data, which were measured at 1 A/m^2 . For 100 keV ions, the measured blistering threshold at room temperature is $0.4 \times 10^{22} \text{ m}^{-2}$, that is less than the value given in [7] for deuterium ions, which is $1.4 \times 10^{22} \text{ m}^{-2}$. For D/H ions, the isotope effect of blistering is known to be about the factor of 2. The other possible reasons of this difference are the particular features of material properties, the processing and the irradiation regime.

Initial formation of blisters occurs at defects of the material. In some experiments with low-dose irradiation of hot targets we observed well-ordered arrangement of blisters (Fig. 5a) that follows the tracks of diamond cutter during the processing. Note that such defects were not seen in SEM images of the surface before irradiation. Similar patterns were found on the periphery of the exposed zone of the copper targets irradiated by a beam halo in high-fluence experiments.

Flaking was observed in some other experiments with the copper targets exposed to the fluence above $2 \times 10^{22} \text{ m}^{-2}$ and on the

periphery of the beam-irradiated area mainly (Fig. 5b). Estimate of the thickness of the flakes from these images gives $\sim 0.4 \mu\text{m}$.

3.2. Tungsten targets

Behavior of tungsten targets under proton beam irradiation is similar to the copper ones. We use industrial-grade material as supplied, i.e. the surfaces of tungsten targets were not machined before the experiment. Therefore, the use of optical diagnostics was less informative in this case. The intensities of scattered and reflected light change during irradiation because of blackening of the surface, so the effect of blistering was not as clear as with the copper target. Meanwhile, in two experiments with the beam energy of 100 keV, the target temperatures of 300 and 370 K and accumulated fluence of 10^{23} m^{-2} , we estimate the blistering threshold for tungsten in the range of $(2 \div 4) \times 10^{22} \text{ m}^{-2}$.

3.3. Tantalum and vanadium targets

Tantalum and vanadium were considered as blistering-resistant materials. Tantalum targets were studied in several experiments with the beam energies of 100 or 200 keV, the target temperatures of 300 or 370 K and the beam current density of up to 14 A/m^2 . Maximal fluence of $2.3 \times 10^{24} \text{ m}^{-2}$ was accumulated in the regime with the beam energy of 100 keV and 300 K temperature; this is the worst case according to our experience with the copper target. Blistering threshold was not achieved in any experiment. Comparison of the dynamics of scattered light during the irradiation for the tantalum and copper targets is shown in Fig. 6. Fig. 7a presents SEM images of the target after accumulation of fluence of $2.3 \times 10^{24} \text{ m}^{-2}$. Left-top part of the image was placed in the shadow of the target holder and was not irradiated. Right-bottom darker part of the image is the irradiated surface. The only difference of these parts of the images is some darkening of the irradiated surface. A possible reason of such changes in optical properties is

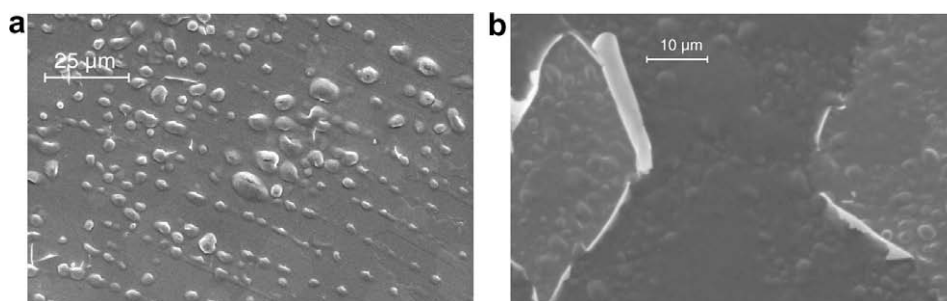


Fig. 5. SEM images of the irradiated copper targets; part (a) is for $E = 190$ keV, $T = 366$ K, fluence $11.4 \times 10^{22} \text{ m}^{-2}$, blisters at the tracks of diamond cut; part (b) is for $E = 96$ keV, $T = 296$ K, fluence $2.4 \times 10^{22} \text{ m}^{-2}$, flaking at the periphery of the irradiated area.

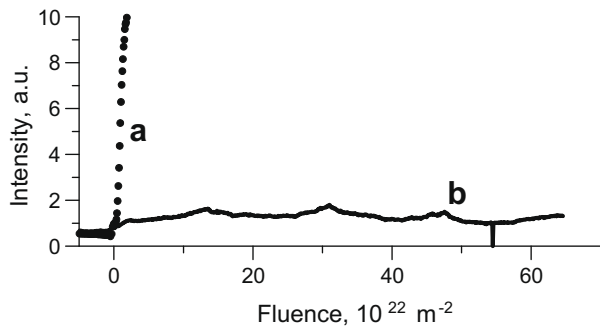


Fig. 6. Dynamics of the scattered light intensities for copper (a) and tantalum (b) irradiated in identical regimes.

the radiation damage effect (DPA value achieves ~ 1000 at fluence of $2.3 \times 10^{24} \text{ m}^{-2}$).

The mentioned fluence corresponds to 40 h of target operation under proton beam with 2.5 A/m^2 current density, this meets the requirements for a target lifetime for the BNCT project [9].

Vanadium was tested in one experiment in the “worst case” regime mentioned above. There was no blistering observed on the target after irradiation up to fluence of $1.2 \times 10^{24} \text{ m}^{-2}$. Thus vanadium (likewise tantalum) is a blistering-resistant material suitable for use in proton-beam-irradiated targets.

3.4. Palladium and iron targets

Two other elements initially considered as a candidate target materials were palladium and iron. Palladium is widely used for treatment with hydrogen. A well-known property of palladium is the so-called “super permeability” that means possibility of palladium membranes to transmit high amounts of hydrogen (see, e.g.,

[10]). Pure iron (α -ferrum) has similar properties. Moreover, it is characterized by extremely low activation energy of hydrogen diffusion (0.045 eV).

In the only experiment, palladium target was irradiated by 100 keV protons up to fluence of $6.7 \times 10^{23} \text{ m}^{-2}$. Some blisters were found on the surface of the irradiated target (Fig. 7b). Estimate of blistering threshold by optical diagnostic gives the value in the range of $(0.8 \div 1.5) \times 10^{23} \text{ m}^{-2}$.

In the experiments with iron targets, blistering appears at the fluence of $(2 \div 3) \times 10^{24} \text{ m}^{-2}$. Fig. 8a shows the surface of the iron target irradiated up to $7 \times 10^{24} \text{ m}^{-2}$ with several generations of broken blisters clearly visible.

Slow sweeping of the beam along the iron target done in one experiment caused flaking of the surface (Fig. 8b). The accumulated fluence was $8 \times 10^{24} \text{ m}^{-2}$ for this experiment. The thickness of flakes measured from the SEM photos is about 200 nm, this is sufficiently less than 200 keV proton penetration depth in iron which is 850 nm.

4. Discussion

According to the theory of blistering [1], the main parameters, which determine the threshold of blistering are: energy of ions, mechanical properties of the irradiated metal and concentration of hydrogen atoms implanted into the target. Secondary effects, which also influence the blistering threshold are accumulation of radiation damages and change of mechanical and structural properties of the target under irradiation. Note that the hydrogen concentration sufficiently depends on current density in contrast to the radiation damages, which are determined by irradiation fluence only.

Physical parameters of the studied materials (taken from [11]) and experimentally measured blistering thresholds are compiled in the Table 1.

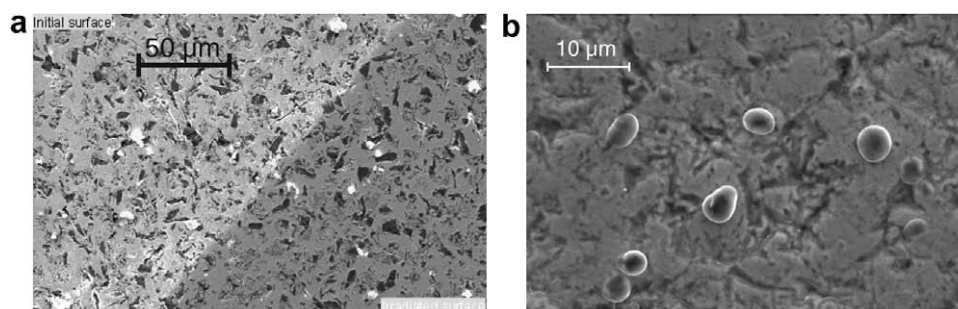


Fig. 7. SEM images of the irradiated surfaces: (a) is tantalum exposed to fluence $2.3 \times 10^{24} \text{ m}^{-2}$, left-top is area shadowed by a target holder (not irradiated), right-bottom is the irradiated area; (b) is palladium target after fluence $6.7 \times 10^{23} \text{ m}^{-2}$.

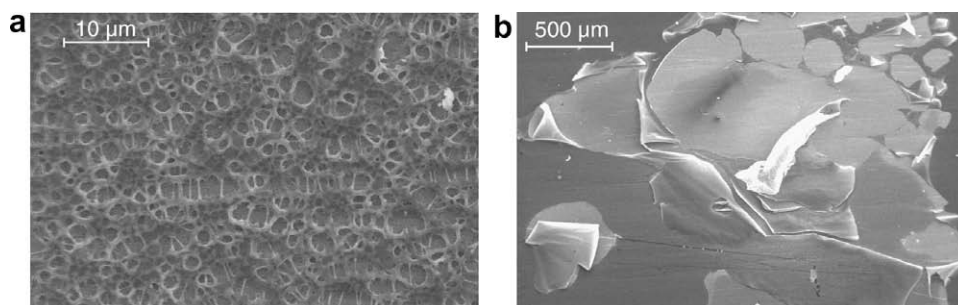


Fig. 8. SEM images of the irradiated surfaces: (a) several generations of broken blisters on the iron surface and (b) flaking of iron target at beam sweeping.

Table 1
Blistering threshold and physical properties of selected materials.

Element	Yield point (10^7 Pa)	Diffusion activation energy, E_D (eV)	Dissolution energy E_S (eV)	Blistering threshold (10^{22} m $^{-2}$)
Cu	20–50	0.4	0.37	0.4–0.1
W	50–90	0.39	1.03	2–4
Fe	12–15	0.05	0.27	80–150
Pd	20	0.23	–0.11	200–300
V	31	0.045	–0.34	Not observed up to 120
Ta	57	0.14	–0.35	Not observed up to 230

The most important parameter that correlates with the blistering threshold is the dissolution energy E_S . Materials with negative dissolution energy (vanadium, tantalum, palladium) are sufficiently more resistant against blistering as compared to other metals.

Copper and tungsten are non-reactive materials, which endothermally dissolve hydrogen. Such materials are characterized by low hydrogen solubility that increases with temperature and by slow diffusion of hydrogen.

Several processes determine spatial distribution of hydrogen in metal during the irradiation. One of them is the diffusion which is different for high-current-density experiments and for the experiments performed at lower beam parameters. Calculated spatial profile of hydrogen concentration in a copper target irradiated by 200 keV, 1 A/m 2 proton beam up to 1.4×10^{22} m $^{-2}$ fluence is shown in Fig. 9. This fluence corresponds to experimentally measured blistering threshold for the beam with the same parameters. Hydrogen diffusivity in copper was taken from [12].

The hydrogen concentration peak is ≈ 40 μ m wide that is sufficiently larger than the beam straggling (≈ 0.13 μ m) and even than the range of 200 keV protons in copper (≈ 1 μ m). This means that Bragg peak is fully smeared by diffusion. Curve (a) in Fig. 9 corresponds to the case of absence of recombination flux from the vacuum surface (full accumulation of the implanted hydrogen). Curve (b) is calculated in the assumption of unlimited flux from the vacuum surface. It should be noted that since the dissolution energy is positive for copper, classical theory of hydrogen desorption [13] predicts very high recombination rates on the surface. In the experiments performed, no special attempt to clean the target surface was made and, therefore, the surface was contaminated. The presence of contamination film sufficiently decreases the desorption flux so it is more probable that in a real target the hydrogen concentration is closer to the upper curve of Fig. 9, i.e. hydrogen accumulates in the target.

According to [3], the tension in a crystal lattice caused by the dissolved hydrogen atoms can be estimated as $\sigma = n_H E_S$, where E_S is dissolution energy of hydrogen in metal and n_H is concentration of hydrogen. If this tension exceeds the yield point of the target

material $\sigma_T = 70$ MPa, a destruction of sub-surface layer occurs. Hence it is possible to estimate relative concentration of hydrogen, which gives rise of blistering:

$$\frac{n_H}{n_{Cu}} = \frac{\sigma_T}{n_{Cu} \cdot E_S} = 0.014.$$

The value of hydrogen concentration at blistering threshold estimated from the diffusion calculations is 0.008. The difference between the prediction and the experiment can be explained by degradation of mechanical properties of the surface layer under irradiation.

Tantalum has negative hydrogen dissolution energy, therefore, it can accumulate large amount of hydrogen. Hydrogen diffusion rate in tantalum is very high, therefore, hydrogen redistributes over the target deeper. The maximal concentration of hydrogen in this case is determined by the equilibrium between the incoming flux of the beam and the outgoing recombination flux from the surface. For a 1-mm-thick tantalum target irradiated by 11.6 A/m 2 proton beam, the equilibrium hydrogen concentration is $\approx 15\%$. Surface contamination strongly decreases hydrogen desorption, thus, the maximal hydrogen concentration can achieve larger values. Moreover, in a real neutron-generating target [9] the surface will be covered by lithium layer that suppresses surface recombination.

The calculated dynamics of hydrogen concentration in tantalum target is shown in Fig. 10. Maximal fluence accumulated in the experiment is 2.3×10^{24} m $^{-2}$; this corresponds to the hydrogen concentration of $\approx 4\%$. The increase of the accumulated dose above 10^{25} m $^{-2}$ requires an additional study of stability of hydrogen-contained target. The closest critical point for tantalum is at the hydrogen concentration of 17%. Accumulation of such amount of hydrogen in tantalum at room temperature leads to the phase transition from the solid solution of hydrogen in tantalum (α -phase) to the ordered tantalum hydride Ta $_2$ H (β -phase) accompanied with re-arrangement of crystal lattice with possible loss of mechanical strength. The dissolved hydrogen also causes expansion of the crystal lattice [12]:

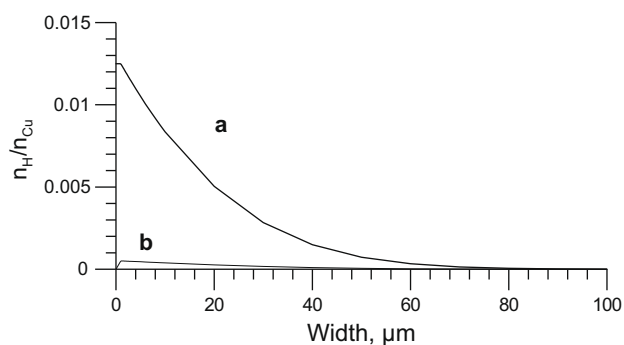


Fig. 9. Calculated spatial distribution of hydrogen atoms in copper target for current density of 1 mA/m 2 and fluence of 1.4×10^{22} m $^{-2}$: (a) is for closed border and (b) is for open border.

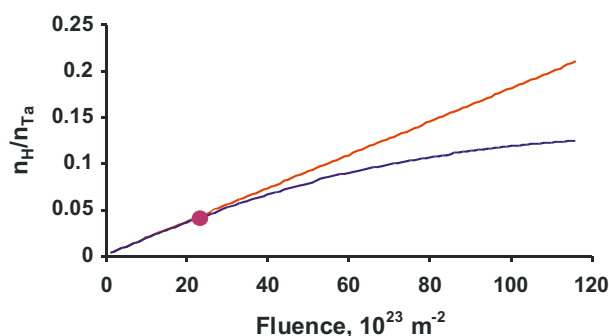


Fig. 10. The hydrogen concentration vs. the fluence for tantalum target of a 1-mm thickness irradiated by proton beam of 100 keV, 11.6 A/m 2 at 300 K; calculations are for (1) full accumulation of hydrogen and (2) for hydrogen desorption from vacuum surface; dot indicates the dose accumulated in our experiment.

$$\Delta L/L = 0.15 \cdot n_H/n_{Ta}$$

and can result in mechanical instability not only of the surface layer but of the whole target.

Generally, it is well known that despite of extensive investigation concerned with the problem of hydrogen energetics, no materials were found able to retain up to 100 ÷ 200% of hydrogen. Therefore, the problem of creation of long-living targets requires extraction of hydrogen through the vacuum or cooling border of the target.

5. Summary

The processes of blistering on several materials irradiated by a high-current–density proton beam were studied. Blisters gradually arise on the surface after some fluence accumulation without sharp threshold of blistering. Regular structure of the blistering formation is observed on Cu and W surfaces. Appearance of blisters depends on the surface condition and the method of its machining.

Tantalum and vanadium are found as the materials most resistant against blistering. Fluence up to $2.3 \times 10^{24} \text{ m}^{-2}$ does not cause blistering for these materials. Extension for acceptable fluence above 10^{25} m^{-2} requires additional studies of target durability.

Acknowledgements

This work was partially supported by Russian Foundation for Basic Research Project 08-02-13570, Russian Ministry of Education Grant RNP 2.1.1/3983, Russian Science Support Fund.

References

- [1] M.I. Guseva, Yu.V. Martynenko, *Soviet Phys. – Uspekhi* 24 (1981) 996.
- [2] R. Behrisch (Ed.), *Sputtering by Particle Bombardment II*, Springer, New York, 1984.
- [3] Yu.V. Martynenko, *Soviet J. Plasma Phys.* 3 (1977) 395.
- [4] S. Taskaev, B. Bayanov, V. Belov, *J. Phys.: Conf. Ser.* 41 (2006) 406.
- [5] A. Kudryavtsev et al., *RSI* 79 (2008) 02C709.
- [6] R. Yadava et al., *J. Phys. D* 13 (1980) 2077.
- [7] T. Armstrong, R. Corliss, P. Johnson, *J. Nucl. Mater.* 98 (1981) 338.
- [8] S. Melnychuk, R. Meilunas, in: *Proceedings of 1999 Particle Accelerator Conference*, vol. 2599, 1999.
- [9] J. Yongen et al., Patent PCT/EP2007/058845, 2007.
- [10] A. Livshitz, *Vacuum* 29 (1979) 103.
- [11] O.V. Ogorodnikova, *J. Nucl. Mater.* 290–293 (2001) 459.
- [12] *Hydrogen Metal Systems, Parts I, II Solid State Phenomena*, vols. 49–50 and 73–75.
- [13] M.A. Pick, K. Sonnenberg, *J. Nucl. Mater.* 131 (1985) 208.